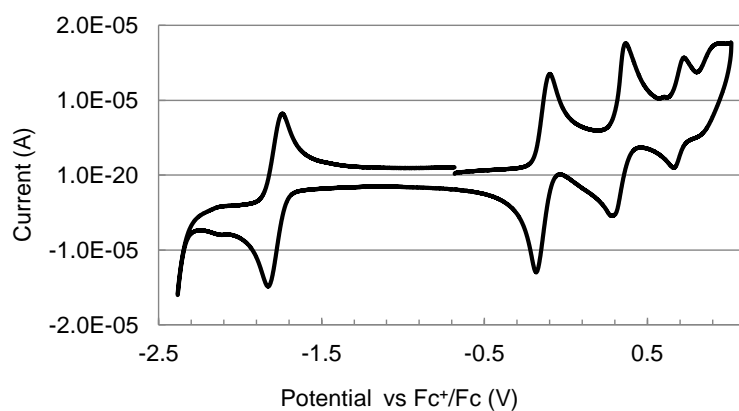


## **Supporting Information**

**Ferrocene-dithiolene hybrids: control of strong donor-acceptor  
electronic communication to reverse the charge transfer direction**

Tetsuro Kusamoto, Kenji Takada, Ryota Sakamoto, Shoko Kume, and  
Hiroshi Nishihara\*



**Figure S1.** Cyclic voltammogram of  $\text{FcS}_4\text{dt}[\text{Pt}(\text{tBu}_2\text{bpy})]$  with a sweep area from -2.4 V to 0.75 V. Condition: 0.1 M  $\text{Bu}_4\text{N}\cdot\text{ClO}_4$  in  $\text{CH}_2\text{Cl}_2$ , room temperature, GC working electrode, Pt counter electrode, scan rate of  $100 \text{ mV}\cdot\text{s}^{-1}$ .

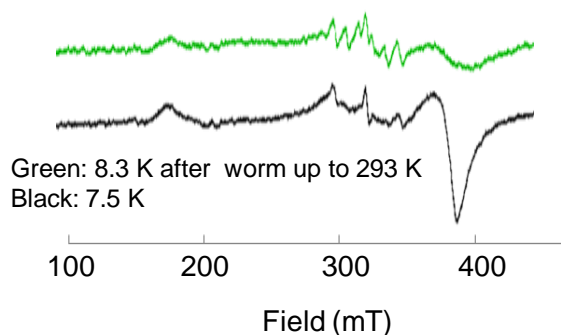


**Figure S2.** EPR spectra of  $[\text{FcS}_4\text{dt}(\text{Me})_2]^+$  in frozen  $\text{CH}_2\text{Cl}_2$  measured at 7.5 K (black line). The sample was warmed up to 293 K and was again cooled down to 8.3 K, at which EPR spectrum was recorded (green line).

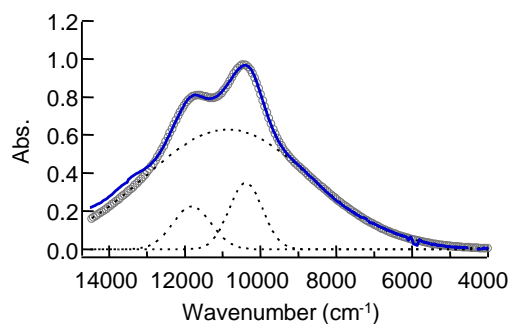


**Figure S3.** Deconvolution of the spectrum of  $[\text{FeS}_4\text{dt}[\text{Pt}(\text{tBu}_2\text{bpy})]]^+$  (blue line) at NIR region. Dotted lines represent Gaussian curves, and gray circles show a sum of the Gaussian curves. It is noted that three Gaussian curves were used to reproduce the obtained spectrum in the range from 12500 to 4000  $\text{cm}^{-1}$  and that the shoulder at 13260  $\text{cm}^{-1}$  were not considered in this deconvolution to avoid over-parameterization.

**Table S1.** Crystal Data and Refinement Parameters for  $\text{FcS}_4\text{dt}(\text{Me})_2$ ,  $\text{FcS}_4\text{dt}[\text{Pt}(\text{tBu}_2\text{bpy})]$ , and  $[\text{FcS}_4\text{dt}[\text{Pt}(\text{tBu}_2\text{bpy})]](\text{F4TCNQ}) \cdot \text{C}_6\text{H}_{14} \cdot \text{CH}_2\text{Cl}_2$

	$\text{FcS}_4\text{dt}(\text{Me})_2$	$\text{FcS}_4\text{dt}[\text{Pt}(\text{tBu}_2\text{bpy})]$	$[\text{FcS}_4\text{dt}[\text{Pt}(\text{tBu}_2\text{bpy})]](\text{F4TCNQ}) \cdot \text{C}_6\text{H}_{14} \cdot \text{CH}_2\text{Cl}_2$
Empirical formula	$\text{C}_{16}\text{H}_{12}\text{FeS}_6$	$\text{C}_{32}\text{H}_{32}\text{FeN}_2\text{PtS}_6$	$\text{C}_{48}\text{H}_{41}\text{Cl}_2\text{F}_4\text{FeN}_6\text{PtS}_6$
<i>F</i> w	452.57	887.90	1292.07
Crystal dimension (mm)	0.30 × 0.10 × 0.10	0.20 × 0.10 × 0.10	0.10 × 0.05 × 0.01
Crystal system	monoclinic	monoclinic	triclinic
Lattice parameters	<i>a</i> = 11.930(3) Å <i>b</i> = 15.096(3) Å <i>c</i> = 19.621(4) Å	<i>a</i> = 14.482(3) Å <i>b</i> = 11.329(2) Å <i>c</i> = 20.162(4) Å	<i>a</i> = 11.320(6) Å <i>b</i> = 12.296(6) Å <i>c</i> = 19.737(10) Å <i>α</i> = 95.252(9)° <i>β</i> = 97.482(10)° <i>γ</i> = 94.938(8)°
	<i>V</i> = 3508(1) Å <sup>3</sup>	<i>V</i> = 3236(9) Å <sup>3</sup>	<i>V</i> = 2699(2) Å <sup>3</sup>
Space group	<i>P</i> 2 <sub>1</sub> / <i>c</i>	<i>P</i> 2 <sub>1</sub> / <i>a</i>	<i>P</i> -1
<i>Z</i> value	8	4	2
<i>λ</i>	0.7107 Å	0.7107 Å	0.7107 Å
<i>T</i>	113 K	113 K	93 K
<i>μ</i> (Mo K $\alpha$ )	1.567 mm <sup>-1</sup>	5.179 mm <sup>-1</sup>	3.241 mm <sup>-1</sup>
<i>D</i> (calc)	1.713 g/cm <sup>3</sup>	1.822 g/cm <sup>3</sup>	1.590 g/cm <sup>3</sup>
<i>R</i> <sub>1</sub>	0.0455	0.0647	0.083
<i>WR</i> <sub>2</sub>	0.1363	0.1004	0.2088
Goodness of fit	1.076	1.123	1.034

**Table S2.** Absorption Wavelengths and Energies of  $\text{FcS}_4\text{dt}(\text{Me})_2$ , and the Corresponding Transition Energies and Oscillator Strengths Calculated by the TD-DFT Method

$\lambda_{\text{max}}^a / \text{nm}$	$E_{\text{max}}^a / \text{eV}$	$E_{\text{calc}}^b / \text{eV}$	Oscillator strength $f^c$	Configuration <sup>d</sup>	coefficient
322	3.85	3.76	0.184	111 ->117	-0.39
				113 ->119	0.35
		3.73	0.0837	111 ->117	0.51
		3.73	0.0203	114 ->120	-0.31
				115 ->120	0.30
374	3.31	3.49	0.0187	113 ->119	-0.34
				113 ->121	0.59
450	2.75	3.00	0.012	113 ->117	0.50
				115 ->119	-0.41
		2.891	0.0086	116 ->119	0.67

a: Absorption maxima.

b: Corresponding transition energy calculated by the TD-DFT method.

c: Oscillator strength calculated by the TD-DFT method.

d: Main contributions (> 0.3) are shown.

**Table S3.** Absorption Wavelengths and Energies of  $\text{FcS}_4\text{dt}[\text{Pt}(\text{tBu}_2\text{bpy})]$  and the Corresponding Transition Energies and Oscillator Strengths Calculated by the TD-DFT Method

$\lambda_{\text{max}}^a / \text{nm}$	$E_{\text{max}}^a / \text{eV}$	$E_{\text{calc}}^b / \text{eV}$	Oscillator strength $f^c$	Configuration <sup>d</sup>	coefficient
630	1.97	1.71	0.129	184 ->185	0.69
393	3.15	2.73	0.0197	183 ->185	0.68
		2.92	0.0107	184 ->188	0.70
		2.94	0.0471	181 ->185	0.67
360	3.44	3.30	0.0561	184 ->189	0.49
				184 ->191	-0.48

a: Absorption maxima.

b: Corresponding transition energy calculated by the TD-DFT method.

c: Oscillator strength calculated by the TD-DFT method.

d: Main contributions (> 0.3) are shown.

**Table S4.** Absorption Wavelengths and Energies of [FcS<sub>4</sub>dt[Pt(<sup>t</sup>Bu<sub>2</sub>bpy)]]<sup>+</sup>, and the Corresponding Transition Energies and Oscillator Strengths Calculated by the TD-DFT Method

$\lambda_{\max}^a / \text{nm}$	$E_{\max}^a / \text{eV}$	$E_{\text{calc}}^b / \text{eV}$	Oscillator strength $f^c$	Configuration <sup>d</sup>	coefficient
920	1.35	1.14	0.0965	183B ->184B	0.99
968	1.28				
852	1.45	1.42	0.2705	181B ->184B	0.96
732	1.69				
580	2.14	2.36	0.0262	184A ->185A	0.94
		2.37	0.01	175B ->184B	0.85
				177B ->184B	0.33
470	2.64	2.73	0.0164	173B ->184B	0.93

a: Absorption maxima.

b: Corresponding transition energy calculated by the TD-DFT method.

c: Oscillator strength calculated by the TD-DFT method.

d: Main contributions (> 0.3) are shown.